ELSEVIER

Polymer 43 (2002) 6273–6279

polymer

www.elsevier.com/locate/polymer

Melting of benzene in a poly(ethyl acrylate) network studied by TMDSC

M. Salmerón Sánchez*, M. Monleón Pradas, J.L. Gómez Ribelles

Center for Biomaterials, Universidad Politécnica de Valencia, Camino de Vera s/n, E-46071 Valencia, Spain

Received 16 January 2002; received in revised form 29 July 2002; accepted 2 August 2002

Abstract

First order transitions of a solvent in a gel differ from those of the solvent alone. In particular, the existence of either several endothermic peaks, or of a broad one is a common feature. In this respect, melting of a solvent sorbed in a polymer matrix presents a phenomenology similar to that of a semi-crystalline polymer. In this work temperature modulated differential scanning calorimetry (TMDSC) has been applied to study the melting behaviour of benzene in a poly(ethyl acrylate), PEA, network. A strong frequency dependence is found both of the real and imaginary part of the complex heat capacity in the transition regions. The kinetic response of the material to the temperature modulation is analyzed with the model proposed by Toda et al., developed for the kinetic melting behaviour of crystalline polymers, which seems to be applicable also to the system studied in this work. © 2002 Published by Elsevier Science Ltd.

Keywords: Temperature modulated differential scanning calorimetry; Kinetics of melting; Sorption

1. Introduction

Temperature modulated differential scanning calorimetry (TMDSC), is a relatively new technique [1,2] that superposes an oscillating temperature profile on a conventional DSC scan. TMDSC has been a useful tool in the study of the glass transition [3–6] and for improving the knowledge about the kinetics of melting and crystallization of polymers [7–12]. For this purpose, the conventional kinetic analysis of first order transitions usually needs certain specific data that most of the times are not available. For example, the Avrami equation [13] involves the morphology of the crystals. Recently Toda et al. proposed an alternative way to manage the problem through a phenomenological model that explains the kinetics of melting and crystallization of polymers based on the evolution of the rate of transformation [14–20]; the model is correlated with TMDSC experiments. This work analyses the application of this model for explaining the kinetic behaviour of the melting of benzene, a non-polar low molecular weight substance, in a PEA network.

Due to the phase lag, φ, between the calorimeter response function (i.e. the heat flow) and the time derivative of the modulated temperature program, a complex apparent heat capacity is defined, C^*, whose modulus is

$$|C^*| = \frac{\dot{Q}_a}{\omega T_a} \tag{1}$$

Here $\dot{Q}_a$ is the amplitude of the first harmonic of the periodic component of the heat flow, T_a is the amplitude of the temperature wave, and ω is the modulation frequency. Thus, data treatment is done through a Fourier analysis that assumes a linear response of the process, i.e. in the case a sinusoidal temperature modulation is programmed a pure sinusoidal response should be obtained in the heat flow. Once these inconveniences have been overcome (selecting the adequate combinations of values of underlying heating rate, frequency and temperature amplitude), three temperature dependent magnitudes are obtained as representatives of a TMDSC experiment [21–23]

$$C_\beta = \frac{\dot{Q}_u}{\beta}, \tag{2a}$$

$$C' = |C^*|\cos\varphi, \tag{2b}$$

$$C'' = |C^*|\sin\varphi. \tag{2c}$$

Eq. (2a) describes the heating rate dependent heat capacity obtained from the underlying component of the heat flow, $\dot{Q}_u$, i.e. the frequency independent component in the Fourier analysis, and is equivalent to the trace of a conventional DSC analysis at the average heating rate, β. Eq. (2b) gives

* Corresponding author. Tel.: +34-96-387-7275; fax: +34-96-387-7276.
E-mail address: masalsan@fis.upv.es (M. Salmerón Sánchez).

0032-3861/02/$ - see front matter © 2002 Published by Elsevier Science Ltd.
PII: S0032-3861(02)00534-7

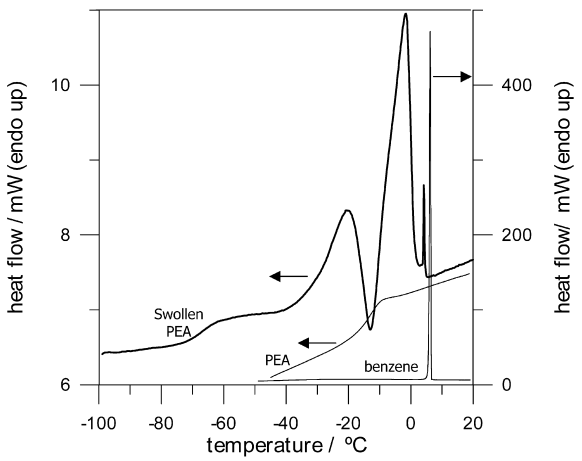

Fig. 1. DSC thermograms, obtained on heating at 10 °C/min after cooling at the same rate, for the pure benzene, PEA and PEA swollen in benzene.

the real part of the complex heat capacity, the component in phase with the heat flow, and Eq. (2c) the imaginary part, the out of phase component that appears when time dependent processes take place in the sample.

Melting of polymer crystals is a complicated phenomenon that has been widely studied by TMDSC. Polymer crystals have a distribution of non-equilibrium melting points [24], which gives rise to a broad endothermic peak in a DSC scan. In this respect the phenomenology of melting of a solvent in a gel is similar to that of a polymer. In particular, for the system studied in this work, on heating in a DSC scan, melting starts a few degrees above the glass transition of the swollen polymer and it continues (there are also processes of recrystallization and reorganization) up to values near the melting temperature of pure benzene [25]. This represents a temperature interval of almost 50 °C, as it is clearly seen in Fig. 1. However, it is well known that melting is a fast process that takes place with low superheating. It seems likely that a fraction of crystals having melting points slightly lower than sample temperature melts in a time interval comparable to the modulation period, and so a frequency response in a TMDSC experiment is expected [18].

This work is a first attempt at understanding the melting kinetics of a solvent absorbed in a gel by TMDSC. A system has been chosen where no polar interaction between the polymer chains and the molecules of the solvent exists. The physical picture could be imagined as that of small crystals of benzene molecules, which form a separate phase, trying to melt and diffuse in a polymer matrix, which is a homogeneous polymer gel.

2. Experimental

A poly(ethyl acrylate), PEA, (monomer from Aldrich 99% pure) network was polymerised via ultraviolet light using ethylenglycol dimethacrylate, EGDMA (Aldrich, 98% pure) as crosslinking agent (1 wt%) and benzoine (Scharlau 98% pure) as photoinitiator (0.13 wt%). Low molecular weight substances were extracted from the polymer network by boiling in ethanol for 24 h and then drying it in vacuum to a constant weight.

Samples for DSC were cut from a PEA network plate and were introduced in a saturated benzene atmosphere at room temperature until equilibrium was reached (weight fraction of benzene, $\text{mass}_{\text{benzene}}/\text{mass}_{\text{swollen gel}}$, 0.51). TMDSC was performed in a Pyris 1 apparatus (Perkin–Elmer). Dry nitrogen gas was let through the DSC cell with a flow rate of 20 ml/min. The temperature of the equipment was calibrated by using indium and benzene. The heat of fusion of indium was used for calibrating the heat flow.

Before the modulated scan, the sample was subjected to a DSC cooling scan from ambient temperature down to −50 °C at a rate of 10 °C/min. The modulated temperature program was a tooth-saw temperature profile with an average heating rate of 1.5 °C/min, 0.1 °C of amplitude and different modulation periods, P (24, 48, 60, 80 s). A modulated base line with the same conditions was performed immediately after each scan and was later subtracted from the measured oscillating heat flow in order to obtain the TMDSC parameters. The temperature programs were selected so as to comply with a heating condition always, i.e.

$$\frac{dT_s}{dt} > 0 \tag{3}$$

This is achieved in the equipment used in this work selecting the adequate input parameters that define the temperature cycle (T_1, T_2, T_3 and β_1), taking into account that

$$T_s(t) = \begin{cases} T_1 + \beta_1 t & \text{for } 0 \le t \le P/2 \\ (2T_2 - T_3) + \dfrac{T_3 - T_2}{T_2 - T_1}\beta_1 t & \text{for } P/2 \le t \le P \end{cases} \tag{4a}$$

$$\beta = \frac{\beta_1(T_3 - T_1)}{2(T_2 - T_1)} \tag{4b}$$

$$T_a = \frac{1}{2}\left(T_2 - \frac{T_1 + T_3}{2}\right) \tag{4c}$$

$$P = \frac{2(T_2 - T_1)}{\beta_1} \tag{4d}$$

Finally, five TMDSC measurements were performed keeping the same period (48 s), temperature amplitude (0.1 °C), but varying the underlying heating rate: 0.75, 1, 1.5, 2, 2.5 °C/min.

3. Results

Fig. 1 shows a conventional DSC scan performed on the system studied in this work at a heating rate of 10 °C/min

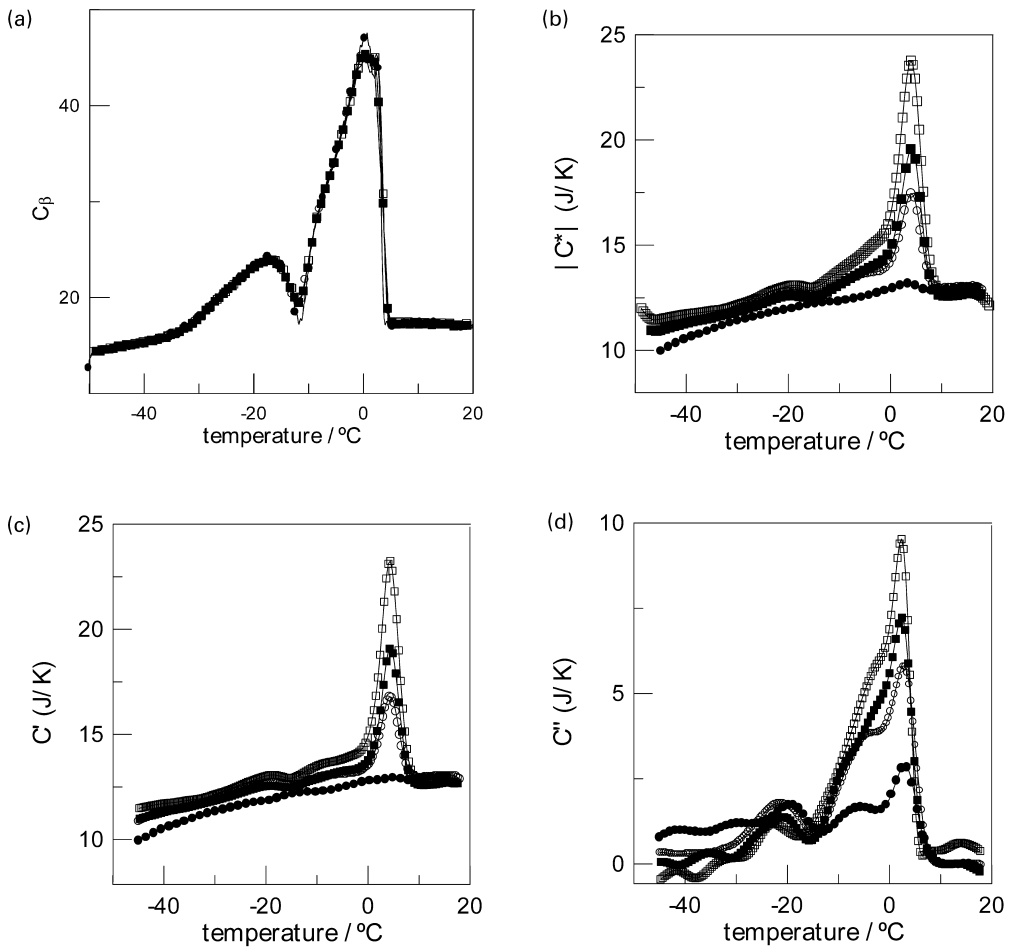

Fig. 2. Results of TMDSC with four different modulation periods, (●) 24 s, (○) 48 s, (■) 60 s, (□) 80 s, versus temperature. (a) Underlying heat capacity, C_β. (b) Magnitude of the complex heat capacity $|C^*|$, real (c) and imaginary (d) parts of the complex heat capacity.

from − 100 °C up to room temperature. The glass transition of the swollen network gel ($T_g \approx -65$ °C) is followed by the melting of benzene which had previously crystallized on cooling. The melting region starts at temperatures immediately above the glass transition, and the TMDSC experiments were performed, based on this result, from − 50 to 20 °C. A sharp peak can be seen in the thermogram of the swollen gel that correspond to melting of benzene that is not homogeneously mixed with the polymer. However, the area of this peak is negligible and so the amount of benzene involved in it.

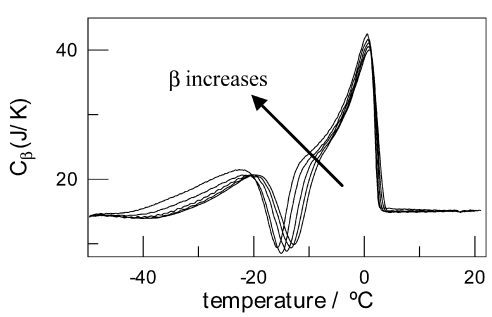

Fig. 3. Underlying component of the heat capacity, C_β, obtained from five TMDSC scan performed with the same modulation period (48 s) and temperature amplitude (0.1 K) and different underlying heating rate: 0.75, 1, 1.5, 2 and 2.5 °C/min.

Fig. 2 shows the TMDSC measurements on heating with four different modulation periods. The heating rate dependent heat capacity, C_β, equivalent to that of a conventional DSC measurement, is depicted in Fig. 2a. Two endothermic peaks separated by an exothermic one are clearly seen. The four curves, corresponding to the four modulation periods used in this work, are superposed, showing, as expected, no frequency dependence. The magnitude of the complex heat capacity is shown in Fig. 2b. A strong frequency dependence is observed, and the magnitude of the peak increases as the frequency is reduced. Finally the real and imaginary parts of the complex specific heat, calculated from the magnitude of the complex heat capacity and the phase lag through Eqs. (2b) and (2c), are displayed in Fig. 2c and d, respectively. Both of them show strong frequency dependence with the same tendency as the magnitude of the complex heat capacity. It is interesting to note that the absolute value of the real part is always higher than the imaginary one, indicating that the phase lag has low values (under 25°). Fig. 3 shows the underlying heat capacity, C_β, obtained from five TMDSC scans with the

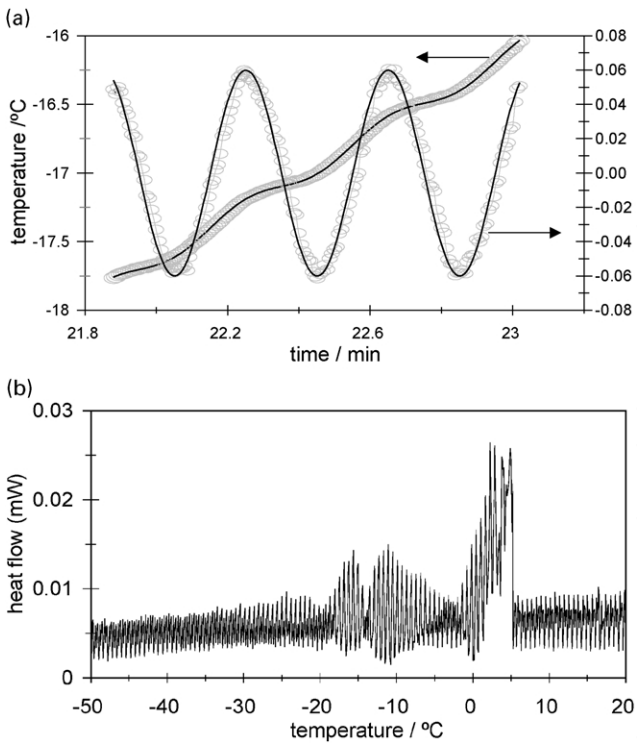

Fig. 4. (a) Comparison of the experimental temperature profile (○) with a sinusoidal function of the same period and amplitude (continuous line). It has been represented, also, the oscillating component of the temperature (i.e. the average heating rate has been subtracted) for a better comparison. (b) Amplitude of the second harmonic of the heat flow. The heating rate was 1.5 °C/min, modulation period 24 s.

same period and temperature amplitude, but modifying the average heating rate.

In respect to the shape of the programmed temperature profile it might be thought that due to the non-sinusoidal waveform a high number of harmonics could be generated, and the analysis would be more difficult. However, for the experimental conditions chosen in this work, the apparatus rounds the cusps of the programmed waveform, and the temperature profile to which finally the sample is subjected is quite similar to a pure sinusoidal: a Fourier analysis of the temperature waveform shows a negligible presence of higher harmonics, as is clearly seen in Fig. 4a, where the experimental sample temperature is compared with a pure sinusoidal of the same frequency. The presence of higher harmonics in the heat flux, though more important than in the temperature wave, which indicates the presence of non-linear phenomena, is also negligible (Fig. 4b), and an analysis of the experimental data based on the linear response theory is adequate.

4. Discussion

Melting of benzene in a PEA network starts a few degrees after the glass transition of the swollen network. As temperature is raised, benzene suffers some process of melting and crystallization on heating and finally melts at a temperature a few degrees lower than the pure solvent does. Fig. 1 shows a melting endotherm that starts at −50 °C but is interrupted by reorganization and crystallization processes that take place in the sample around −15 °C. When these exothermal events (around 5° wide) finish, a large melting peak is observed. It has been checked that the sum of the areas (i.e. enthalpy) of the exothermal peaks (including crystallization on cooling, reorganizations and crystallizations on heating) equals the area of the endothermal ones. However, all these phenomena do not show a frequency dependence when a TMDSC is performed on the sample. Fig. 2b and c show a small low temperature endothermic peak that shows no frequency dependence. For the imaginary part of the specific heat capacity, C'' (Fig. 2d), there is also a small peak at the same temperature interval that is not sensitive to the frequency of the modulated temperature. Exothermal events on heating, i.e. reorganizations and crystallizations, do not show a characteristic trace in the modulated magnitudes. On the contrary, the final melting, at higher temperatures, of the crystallites present in the sample (coming from crystallizations on cooling and on heating) shows a strong frequency dependence both of the magnitude of the specific heat capacity (Fig. 2b) and of the phase lag between the modulated temperature and the heat flow (not shown). This gives rise to a frequency-dependent peak in the real and imaginary parts of the specific heat (Fig. 2b and c). The frequency dependence of the high endothermic peak and the lack of frequency dependence of the low endothermic peak and the exothermal peak can be followed numerically through the evolution of the peak height at different frequencies and it has been resumed in Table 1. The analysis of the frequency dependence of this peak can provide information about the kinetics of the melting process. It seems that the exothermal events on heating are, to a great extent, independent of frequency. Fig. 3 shows five curves corresponding to the underlying linear part of the TMDSC scan (C_β) performed at the same frequency and temperature amplitude but varying the underlying heating rate. The shift of the low temperature region of the curves to lower temperatures is due to crystallizations on heating and reorganizations, and it

Table 1
Peak height of the high endothermic frequency dependent peak and of the two lower frequency independent peaks (endothermic and exothermic) for the real and imaginary parts of the complex heat capacity

Period (s)	High endothermic peak		Low endothermic peak		Exothermic peak	
	C' (J/K)	C'' (J/K)	C' (J/K)	C'' (J/K)	C' (J/K)	C'' (J/K)
24	12.86	2.88	12.14	1.75	11.96	0.99
48	16.81	5.83	12.70	1.79	12.62	0.93
60	19.12	7.22	12.52	1.37	12.51	0.97
80	23.20	9.52	13.01	1.29	12.87	0.89

coincides with the region of the curve that is not sensitive to frequency. However, the high temperature endothermal peak is not heating-rate dependent (Fig. 3) and corresponds to the region where strong frequency dependence was found. The phenomenological model developed by Toda et al. [18] can be an adequate tool for understanding this behaviour. A brief exposition of the model follows, particularized for this system, and a discussion of its application and interpretation.

Let $F(t)$, where t is time, be the part of the heat flow supplied by the calorimeter that is not inverted in rising the temperature of the material but in the phase transformation process. That is, if $\dot{Q}$ is the total heat flow to the sample, it holds

$$\dot{Q} = mc_p \frac{dT_s}{dT} + F(t). \tag{5}$$

$F(t)$ can be expanded about the sample temperature for a small temperature modulation,

$$F(t, T_s) = \bar{F}(t, \bar{T}_s) + F'_T(t, \bar{T}_s) T_a \, e^{i(wt+\varphi)} \tag{6}$$

where $\bar{F}$ represents the heat flow of the phase transformation, i.e. that would be obtained in a conventional DSC analysis at the average heating rate, and $\bar{T}_s$ is the temperature that the equivalent DSC scan would have at that time, i.e. $\bar{T}_s = T_0 + \beta t$.

Let $\phi(t, T_m)dT_m$ be the fraction of crystallites having, at time t, the melting temperature in the range from T_m to $T_m + dT_m$. The endothermic heat flow of melting can be expressed as

$$F = \Delta H \frac{d}{dt} \int_0^\infty \phi(t, T_m) dT_m \tag{7}$$

where ΔH is the total enthalpy change of the system on melting. The model proposed by Toda et al. assumes that the evolution in time of $\phi(t,T_m)$ is controlled by a melting rate coefficient, R, that is a function of superheating, $\Delta T = T_s - T_m$

$$\frac{d\phi(t, T_m)}{dt} = -R(\Delta T)\phi(t, T_m) \tag{8}$$

Solving this equation, with a concrete expression for the superheating dependence of R, allows obtaining via Eq. (6) an expression for the heat flow of transformation, which can be related to the complex heat capacity through its first harmonic in the Fourier expansion.

Since the heating run satisfies the condition of superheating always (Eq. (3)), crystallization cannot be due to temperature drops during the modulated heating scan. Besides, the model does not consider the presence of recrystallization or reorganization of the crystallites. In the case of melting of polymer systems the response of those processes to temperature modulation is expected to be much smaller than that of melting [18,24]. For the system studied in this work there is an exothermic peak during the heating scan, as it is clearly seen in Fig. 1. However, there is almost no frequency response of this phenomenon in the complex heat capacity (Fig. 2b) and our interest is focused at analyzing the zone of the thermogram that shows a strong frequency dependence, that is, the final melting of the crystals in the sample that have been formed either on cooling, on heating or due to recrystallizations and reorganizations at lower temperatures. Under these conditions Eq. (7) can be applied, and its solution is

$$\phi(t, T_m) = \phi_0 \exp\left[- \int_0^t R \, dt' \right], \tag{9}$$

where ϕ_0 is the initial distribution of crystallite fractions that is assumed to be uniform. On this basis, considering the linear expansion of the melting rate coefficient, R, for small temperature modulation, F'_T is calculated introducing the expression obtained via Eq. (9) for $\phi(t,T_m)$ through the expanded R into Eq. (7) and considering the first harmonic of its Fourier series. In this way one obtains [14–16]

$$C^* = mc_p + \frac{i}{\omega} F'_T(\omega), \tag{10}$$

where the expression for $f(\omega) = (i/\omega)F'_T(\omega)$ is [18]

$$f(\omega) = \Delta H \phi_0 \beta \int_0^\infty e^{-i\omega x} \left[e^{-\int_0^x R(\beta y) dy} \int_0^x R'(\beta y) e^{i\omega y} \, dy \right] dx. \tag{11}$$

Depending on the superheating dependence of the melting rate coefficient, the kinetic response will change. Following Toda et al. [18–20] three different expressions have been tested. The first of them is the case of a constant rate coefficient, independent of superheating ($R = R_0$), the second one is a linear dependence of the melting rate on superheating ($R = a\Delta T$), and the third one is an exponential dependence ($R = (a/c)(e^{c\Delta T} - 1)$). The last one is the most general of the three and includes the other two as special cases. Introducing the exponential dependence in Eq. (11), the following expression is obtained

$$f(\omega) = \frac{\Delta H \phi_0}{1 + i\omega\tau_2} \frac{1}{\tau_3} \int_0^\infty (e^{x/\tau_2} - e^{-i\omega x}) \exp\left[- \frac{\tau_2}{\tau_3} \left(e^{x/\tau_2} - 1 - \frac{x}{\tau_2} \right) \right] dx \tag{12}$$

where

$$\tau_2 = \frac{1}{\beta c}, \qquad \tau_3 = \frac{c}{a}$$

(It must be here remarked that in Refs. [18,19] this equation is printed with a mistake.)

It is easy to show that when $\tau_2 \gg \tau_3$ the frequency response corresponds to a linear dependence of the melting coefficient on superheating, and that it corresponds to a constant value of R in the case when $\tau_3 \gg \tau_2$.

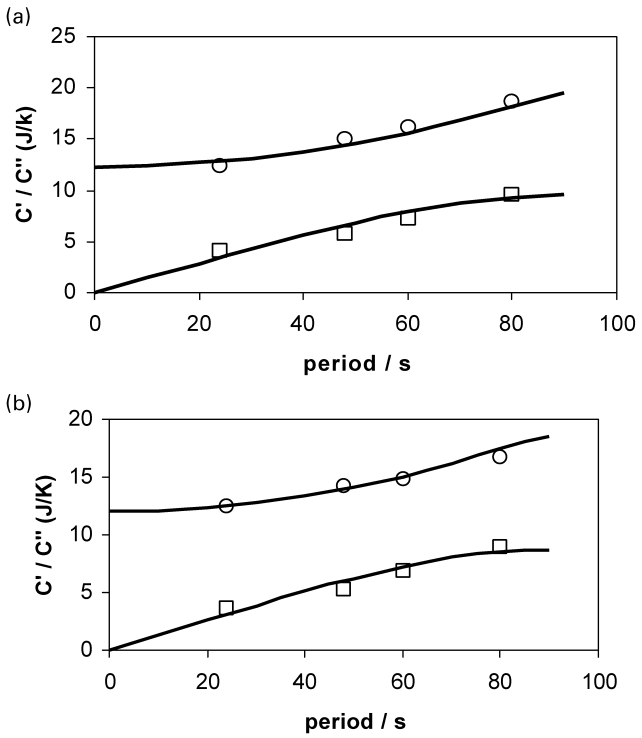

Fig. 5. Real (○) and imaginary (□) part of the complex heat capacity versus the modulation period at two different temperatures (a) 0 °C, (b) 4 °C. The underlying heating rate was 1.5 °C/min. The continuous line corresponds to Eq. (10) with the adjustable parameters c_p, ϕ_0, τ_2 and τ_3.

Fig. 5 shows the frequency dependence of the real and imaginary parts of the complex heat capacity obtained at two different temperatures. The experimental points have been adjusted to the three different kinetic response functions corresponding to the above mentioned superheating dependence of the melting rate. The fit was not good in the case of constant and linear dependence (results not shown), and it was satisfactory for the exponential dependence of the melting rate coefficient. The temperatures chosen in Fig. 5 are representative of the melting interval taking into account that several fits to the Toda model of the experimental data were made in the temperature range of the frequency dependent endothermic peak (the same exponential dependence was found) and the width of the peak (from −2 to 7 °C). Fitting an expression for $f(\omega)$ to the experimental results implies to find a set of parameters (c_p,ϕ_0,τ) that reproduces, at the same time, and for a fixed temperature, the real and imaginary kinetic response of the material. This has been impossible for the kinetic functions obtained for a constant and linear dependence of the melting rate coefficient, consistently with the values of the parameters, τ_2 and τ_3, found in the fitting procedure to Eq. (12). Since the values found for τ_2 and τ_3 are quite similar in each fitting, it is not possible to simplify Eq. (12) to that corresponding to a constant or linear dependence of the transformation rate. An important consequence of this is that the heating-rate dependence of the characteristic time does not depend on temperature, and

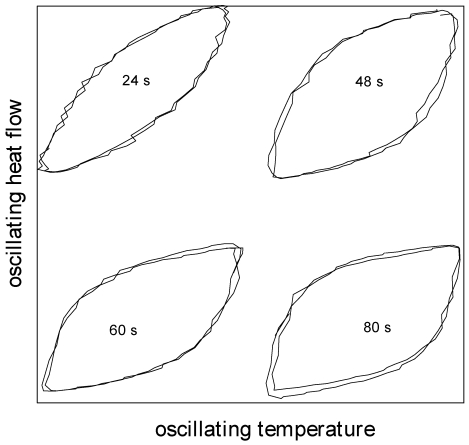

Fig. 6. Lissajous diagrams of two cycles of the modulated component of the heat flow versus the modulated component of the temperature obtained from the high temperature melting region. The average heating rate was 1.5 K/min, the period is indicated in each diagram.

$\tau \propto \beta^{-1}$. This is no longer the case in polymer systems where at higher temperatures the dependence can be fitted to $\tau \propto \beta^{-1}$ while at lower temperatures $\tau \propto \beta^{-1/2}$ (what corresponds to a linear dependence of the melting rate coefficient). The exponential dependence of the melting rate coefficient on superheating in this case of benzene contrasts with the linear dependence found for this magnitude in the case of melting of polymer crystallites. This means that, in the case of the low molecular weight benzene, melting is a faster process than melting of polymers. Melting of a macromolecule implies the disordering of larger structures, and thus longer times are needed when compared to our system, where achieving the liquid state seems a priori easier. On another hand, the exponential dependence of R on ΔT found for melting of benzene in the polymer matrix means a still much lower rate than for melting of pure benzene, for which the present model would hardly be applicable since it would correspond to $R \rightarrow \infty$.

As a consistency test of the linear response achieved in the steady state, needed for the application of the model, Lissajous diagrams of the modulated heat flow against the modulated sample temperature showing a couple of cycles in the melting area have been represented in Fig. 6, which gives the diagrams in the melting region corresponding to the four modulated periods used in this work at the same heating rate. A closed loop can be observed in all cases.

5. Conclusions

Melting of benzene in a PEA network shows two endothermic peaks separated by an exothermic one that correspond to melting and crystallization of the solvent in the polymer matrix as the temperature is raised. Both the low temperature endothermic peak and the exothermal one show no frequency dependence and appear superposed

when a TMDCS is performed. On the contrary, the final melting process shows a strong frequency dependence that can be explained on the basis of the phenomenological model proposed by Toda et al. [18] for polymer systems, based on the dependence on superheating of the melting rate coefficient, R, for each fraction of crystallites. An exponential dependence of R on superheating has been found, what confirms that melting of benzene absorbed in a polymer matrix is faster than the process of melting of crystalline polymers (where a linear dependence has been found for R).

A strong frequency dependence was found for those temperatures where no exothermal phenomena was found on heating. Exothermal events on heating either do not depend on frequency or their frequency response cannot be revealed by the TMDSC technique.

Acknowledgements

Authors acknowledge the support of CICYT through the MAT99-0509 project.

References

[1] Reading D, Elliot D, Hill VL. J Thermal Anal 1993;40:949–55.
[2] Schawe JEK. Thermochim Acta 1996;271:127–40.
[3] Hutchinson JM, Monserrat S. J Thermal Anal 1996;47:103–16.
[4] Hutchinson JM, Monserrat S. Thermochim Acta 1996;286:263–96.
[5] Salmerón M, Torregrosa C, Vidaurre A, Meseguer Dueñas JM, Monleón Pradas M, Gómez Ribelles JL. Colloid Polym Sci 1999;277:1033–40.
[6] Kim SI, Pyo SM, Ree M. Macromolecules 1997;30:7890–7.
[7] Wurm A, Merzlyakov M, Schick C. Colloid Polym Sci 1998;276:289–96.
[8] Schawe JEK, Strobl GR. Polymer 1997;39:3745–51.
[9] Schawe JEK, Bergmann E. Thermochim Acta 1997;304/305:179–86.
[10] Sauer BB, Kampert WG, Neal Blanchard E, Threefoot SA, Hsiao BS. Polymer 2000;41:1099–108.
[11] Merzlyakov SC, Wunderlich B. Pol Bull 1998;40:297–303.
[12] Okazaki I, Wunderlich B. Macromolecules 1997;30:1758–64.
[13] Wunderlich B. Crystal nucleation, growth, annealing. Macromolecular physics, vol. 2. New York: Academic Press; 1976.
[14] Toda A, Oda T, Hikosaka M, Saruyama Y. Thermochim Acta 1997;293:47–63.
[15] Toda A, Oda T, Hikosaka M, Saruyama Y. Polymer 1997;38:231–3.
[16] Toda A, Tomita C, Hikosaka M, Saruyama Y. Polymer 1997;38:2849–52.
[17] Toda A, Tomita C, Hikosaka M, Saruyama Y. Polymer 1998;39:1439–43.
[18] Toda A, Tomita C, Hikosaka M, Saruyama Y. Polymer 1998;39:5093–104.
[19] Toda A, Arita T, Tomita C, Hikosaka M. Thermochim Acta 1999;330:75–83.
[20] Toda A, Saruyama Y. Polymer 2001;42:4727–30.
[21] Schawe JEK. Thermochim Acta 1995;261:183–4.
[22] Schawe JEK. Thermochim Acta 1997;304/305:111–9.
[23] Schawe JEK, Höhne GWH. Thermochim Acta 1996;287:213–23.
[24] Wunderlich B, Macromolecular physics, vol. 3. New York: Academic Press; 1976.
[25] Salmerón Sánchez M, Monleón Pradas M, Gómez Ribelles JL. J Non-Cryst Solids 2002;307/310:750–7.